Pure amplitude and wavelength modulation spectroscopy for detection of N_2O using a three-sections quantum cascade laser

Pietro Patimisco[a,b], Angelo Sampaolo[a,b], Yves Bidaux[c], Alfredo Bismuto[c], Marshall Scott[d], James Jiang[d], Frank K. Tittel[b], and Vincenzo Spagnolo[a]

[a]Dipartimento Interateneo di Fisica, University and Politecnico of Bari, CNR-IFN UOS BARI, Via Amendola 173, Bari, Italy;
[b]Department of Electrical and Computer Engineering, Rice University, 6100 Main Street, Houston, TX 77005, USA;
[c]Alpes Lasers SA, CH-2072 Saint-Blaise, Switzerland
[d]Thorlabs, 10335 Guildord Rd. Jessup, MD 20794

ABSTRACT

We report on a novel quantum cascade laser (QCL) capable of operating in pure amplitude or wavelength modulation configuration thereby allowing the acquisition of background-free gas absorption-line profiles using quartz-enhanced photoacoustic spectroscopy (QEPAS). The QCL is composed of three electrically independent sections: Gain, Phase (PS) and Master Oscillator (MO). The non-uniform pumping of these three QCL sections allows laser wavelength tuning with constant optical power and vice-versa. Pure QEPAS amplitude modulation operating conditions were obtained by modulating the PS current, while pure wavelength modulation was obtained by modulating the MO section and slowly scanning the PS current.

Keywords: quartz tuning fork, photoacoustic spectroscopy, quantum cascade laser, gas sensing

1. INTRODUCTION

The combination of single-mode emission and mode-hop free tunability makes quantum cascade lasers (QCLs) extremely suitable for sensitive and selective trace-gas detection. High detection sensitivities can be achieved by implementing a wavelength modulation (WM) technique in the kHz-frequency range, which reduces the *1/f*-noise originating mainly from laser intensity fluctuations and mechanical instabilities. In WM, the laser frequency is simultaneously modulated by a ramp wave of sub-Hz frequency to the temperature or current control and a sine wave of kHz frequency to the current control. This produces multiple harmonics in the transmitted intensity that a lock-in amplifier can detect. In other words, a WM scheme enables detection of an absorption profile at selected frequencies. However, the modulation of the current produces also modulation of the emitted output power at the same frequency. The origin of this residual amplitude modulation (RAM) in WM and its distorting effects on various harmonic signals has been studied in detail in several papers [1-4]. The RAM gives rise to a high background signal in *1f*-detection with a small absorption signal superimposed. To circumvent the problem of high background signals, detection at twice the applied modulation frequency (*2f*-detection) has been favored, although the RAM contribution distorts the acquired signal [5]. In fact, with *2f*-detection, the acquired Lorentzian gas-absorption profile exhibits a second-derivative lineshape with two unbalanced minima due to the RAM contribution. In order to address the problem, electronic cancellation of RAM has also been attempted by several authors [6, 7]. Recently, a fiber-optic technique capable to eliminate the concentration-independent RAM component at the optical level was also reported [8].
While WM with *2f*-detection has the advantage to be background-free, it does not reproduce the actual absorption profile of a gas line. The WM approach requires post-processing integration of a near-pure first harmonic derivative signal (with *1f*-detection) to recover the gas absorption line shape. An appropriate choice of the lock-in detection phase is needed as well [9]. Recently, a method for recovering absolute absorption line shapes from noisy environments based on pure amplitude modulation from an external lithium niobate amplitude modulator was proposed [10]. The overall signal-to-noise ratio is comparable to that of conventional second harmonic WM, but the apparatus is quite complex.
In this work, we employed a novel QCL source allowing modulation of the laser intensity and frequency independently

Quantum Sensing and Nano Electronics and Photonics XIV, edited by Manijeh Razeghi,
Proc. of SPIE Vol. 10111, 1011109 · © 2017 SPIE · CCC code: 0277-786X/17/$18
doi: 10.1117/12.2252352

of each other. The QCL structure is composed of three electrically independent sections: the gain, the Phase (PS) and the Master Oscillator (MO) section. The QCL was employed in a quartz-enhanced photoacoustic spectroscopy (QEPAS) sensor [11, 12] for the acquisition of a N_2O absorption line. When the PS current is modulated, the optical power is also modulated, while the emission wavelength remains constant. With this condition, a pure amplitude modulation (AM) configuration is achieved. By adding a voltage signal to the MO section QEPAS background-free Lorentzian line-shape spectra were obtained for the targeted N_2O absorption line. When the MO current is modulated, the PS current can be adjusted in order to maintain constant the optical power during modulation. In this manner, a pure wavelength modulation, without any RAM contribution is obtained and the QEPAS spectra show a second-derivate Lorentzian function lineshape. To demonstrate the achievement of a pure WM and AM operating conditions, we implemented the QCL in a quartz enhanced photoacoustic sensor (QEPAS) and selected N_2O as the target gas.

2. AMPLITUDE MODULATION AND WAVELENGTH MODULATION SPECTROSCOPY

Amplitude modulation (AM) spectroscopy is the simplest realization of a laser-based absorption technique. A beam of a tunable laser is sent through a gas sample and the transmitted intensity is measured with a detector. A mechanical chopper modulates the light intensity at certain frequency. The detector signal is then demodulated at the chopping frequency by using a lock-in amplifier. The concentration of the absorbing species can be calculated from the relative change of the intensity according to Lambert-Beer's law. The drawback of this simple technique is that its sensitivity is limited by *1/f*-frequency noise. However, its influence can be greatly reduced by shifting the detection to higher frequencies, in the kHz range. If the laser frequency is scanned across the absorption feature of the target species, the typical Lorentzian-like profile of the gas absorption line can be recovered. Despite the simplicity of the technique and the possibility to recover the actual absorption profile of a gas line, AM spectroscopy has several disadvantages when implemented in a QEPAS setup: i) the absorption signal is small and is positioned on a high background. Usually, a normalization technique is used to extract the small absorption signal from the high background noise; ii) QEPAS requires frequencies in the kHz range and commercially available optical choppers in such a frequency range have a frequency resolution of 1 Hz, much larger than the frequency band typical of quartz tuning forks resonances. Indeed, QEPAS requires a frequency stabilization of at least 0.01 Hz [13-17]; iii) optical choppers in the kHz range are quite noisy, adding a significant noise contribution to the detected QEPAS signal.

Wavelength modulation (WM) spectroscopy is usually accomplished by modulating the QCL injection current, while the wavelength emission is slowly tuned through an absorption feature of the target species to be detected by increasing (or decreasing) the injected current. This current modulation produces changes of the emitted optical power and wavelength, thus leading to a combined wavelength modulation and intensity modulation of the QCL, with a phase difference between the two modulations. There is no means to separate these two effects when the injection current is modulated. The theoretical description is based on the instantaneous laser frequency:

$$\upsilon(t) = \upsilon_0 - \Delta\upsilon\cos(\omega t + \psi) \tag{1}$$

where υ_0 is the optical carrier frequency and $\omega = 2\pi f$ is the modulation angular frequency of the laser frequency due to the laser current modulation occurring at the same angular frequency and ψ is the initial phase. This produces a sinusoidal modulation of the laser intensity P at the same angular frequency:

$$P(t) = P_0 - \Delta P\cos(\omega t) \tag{2}$$

A Taylor-series expansion of the absorption line-shape $\alpha[\upsilon(t)]$ for a small $\Delta\upsilon$ gives:

$$\alpha[\upsilon(t)] = \alpha_0 + \alpha'(\upsilon_0)\Delta\upsilon cos(\omega t + \psi) + \frac{1}{2}\alpha''(\upsilon_0)(\Delta\upsilon)^2 cos^2(\omega t + \psi) \tag{3}$$

where α_0 can be considered to be the background absorption contribution. The laser light transmitted through a weakly absorbing simple according to Lambert-Beer's law for a pathlength L is given by:

$$P_t(t) = [P_0 + \Delta P\cos(\omega t)]\left[1 - \alpha(\upsilon_0)L - \alpha'(\upsilon_0)\Delta\upsilon\cos(\omega t + \psi)L - \frac{1}{2}\alpha''(\upsilon_0)\Delta\upsilon^2\cos^2(\omega t + \psi)L\right] \tag{4}$$

The signal demodulated at twice the modulation frequency f (*2f*-signal) becomes:

$$S_{2f} = -\Delta P \alpha'(\upsilon_0)\Delta\upsilon L + \frac{1}{4} P_0 \alpha''(\upsilon_0)\Delta\upsilon^2 \quad (5)$$

The *2f*-signal is background-free and consists of two terms: the first term is proportional to the first derivative of the absorption and depends on the amplitude of the intensity modulation (residual amplitude modulation, RAM, term), whereas the second term represents the second-derivative term, arising directly from the wavelength modulation. As a result, the demodulated *2f*-signal related to gas absorption line results in a second derivative shape of a Lorentzian profile, with two unbalanced minima due to the RAM contribution.

3. EXPERIMENTAL SETUP

A photo of the QEPAS sensor is shown in Fig. 1a.

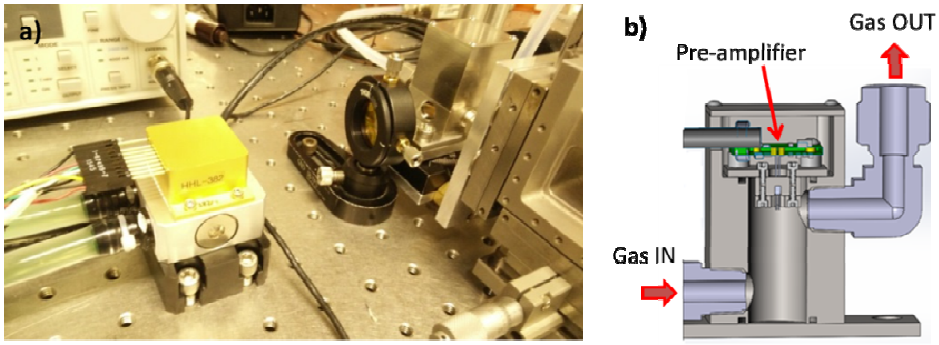

Figure 1. (a) Photo of the QEPAS sensors. The QEPAS sensor consists of a custom QCL, a focusing lens and the QEPAS housing containing both the QTF and the pre-amplifier chip. (b) Sketch of the QEPAS housing designed and realized by Thorlabs, Inc.

The laser source employed in this work was designed and realized by Alpes Lasers S.A. The structure is composed of three independent electrically separated sections: a central Gain section, a Master Oscillator (MO) and a Phase section (PS). The QCL active region design is based on a 2-phonons transition and a detailed description was reported in [18-20]. Each section was separately driven by means of distinct current drivers (ILX Lightwave LDX-3232). When the current I_{MO} in the MO section is varied and the phase section current I_{PS} is kept constant, the frequency of the QCL changes. Conversely, when I_{PS} is varied and the I_{MO} is kept constant, the QCL frequency remains constant. The QCL was operated at a temperature of 10 °C and the Gain section was driven with a fixed current of 800 mA. The radiation of the QCL was directly focused between the prongs of the prong of the quartz tuning fork (QTF) by means of a lens, with a focal length of 50 mm. The prong of the QTF is 17 mm long, 1 mm wide and 0.25 mm thick. The spacing between the two prongs is 0.7 mm [21-23]. The QTF was enclosed in a housing equipped with two ZnSe windows, realized by Thorlabs, Inc (Fig. 1b). The housing contains also the pre-amplifier chip for the QTF signal readout in order to minimize the electrical noise. The QTF signal is then demodulated by means of a lock-in amplifier. The housing was filled with a certified gas mixture composed by 1% of N_2O in pure N_2 at a gas pressure of 85 Torr. The pressure in the enclosure is regulated by a vacuum pump, a pressure controller (MKS, type 649A) and a valve system (not shown in Fig. 1a).
The QTF resonance curve at 85 Torr is depicted in Fig. 2.

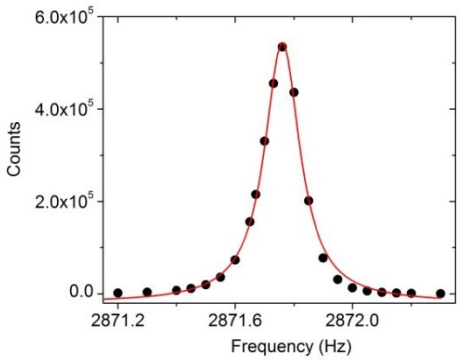

Figure 2. Resonance curve (dots) of the QTF measured at a fixed excitation level of 0.5 mV and at a pressure of 85 Torr with a certified gas mixture composed of 1% of N_2O in pure N_2. The dashed line is a Lorentzian fit.

The QTF resonance frequency f_0 = 2871.76 Hz and the related quality factor Q = 12,400 was deduced from the Lorentzian fit. By using a Fourier-transform interferometer (Nicolet 8700, ThermoScientific) with a spectral resolution of 0.125 cm^{-1} we found that when I_{MO} = 532.1 mA, the laser wavenumber is located at 1278.1 cm^{-1} (as reported in the inset of Fig. 3), resonant with the selected N_2O absorption line having a line strength of $1.18 \cdot 10^{-19}$ cm^{-1}/mol [24]. The PS current is scanned from 0 to 150 mA] keeping I_{MO} fixed at 532.1 mA. We also verified that the QCL emission wavelength does not change in the investigated PS current range. The optical power is reported in Fig.3 as a function of I_{PS}.

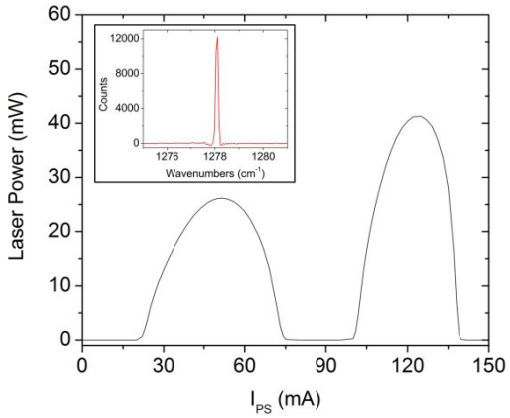

Figure 3. Optical power emitted by the QCL as a function of the PS current (I_{MO} = 532.1 mA and gain section current of 800 mA) measured by means of a power meter. Inset: QCL emission spectrum obtained at I_{MO} = 532.1 mA, I_{PS} = 120 mA and gain section current of 800 mA by using a Fourier-transform interferometer.

The far field mode profile of the laser beam at different PS while I_{MO} was fixed to 532.1 mA was recorded by means of an infrared pyro-camera (Pyrocam III, Ophir Spiricon, 124 x 124 pixels, spatial resolution of 100 μm), positioned at a distance of about 4 cm from the QCL. Representative beam profiles are depicted in Fig. 4.

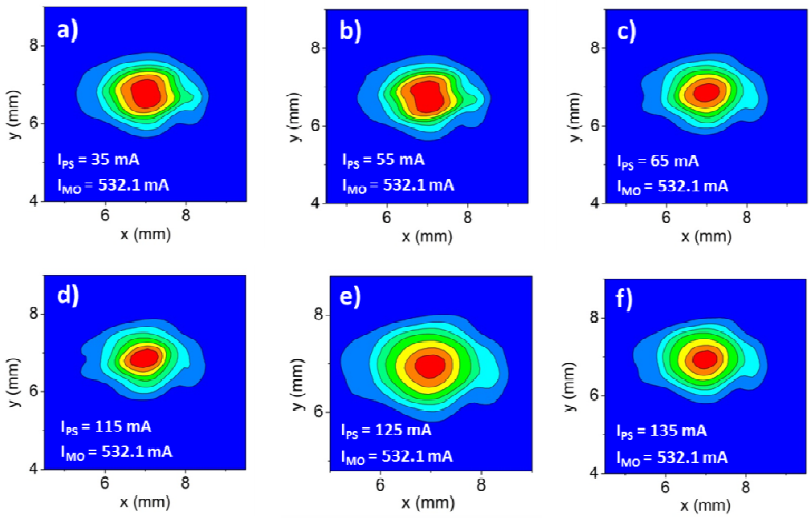

Figure 4. (a-f) Beam profiles of the QCL recorded by positioning the infrared pyro-camera 4 cm away from the QCL exit at i_{PS} = 35 mA (a), 55 mA (b), 65 mA (c), 115 mA (d), 125 mA and 135 mA (f). In all cases the master oscillator current and the gain section current were fixed to 532.1 mA and 800 mA, respectively.

We observed that while the PS current varying from 0 to 150 mA both the spatial quality of the profile and its size are preserved.

4. PURE WAVELENGTH MODULATION

The standard wavelength modulation with *2f* signal acquisition was carried out by modulating the current of the MO section at a frequency $f_0/2$ = 1435.88 Hz, while demodulating the QTF electrical signal at f_0. The current of the PS section was fixed at 120 mA. The spectral scan of the N_2O absorption line was obtained by applying a slow voltage ramp to the MO section at a frequency of 20 mHz. The optimized current modulation depth was b = 2.7 mA, corresponding to a wavenumber modulation depth of 0.029 cm^{-1} [25]. The obtained spectral scan is shown in Fig. 5a. It is background-free and exhibits a second derivative line-shape of a Lorentzian absorption profile. A distortion is apparent in the asymmetry of the two negative lobes surrounding the peak caused by the RAM contribution.

As pointed out in the first term of Equation (5), the RAM term is proportional to the optical power variation ΔP induced by the current modulation. In order to obtain the condition ΔP = 0, two requirements must be satisfied: i) while the MO current varies, the PS current must be adjusted point-by-point in order to obtain a fixed value of the optical power during the scan and ii) a sinusoidal dither must be applied both to the MO and the PS sections. For the former condition, we recorded the trend of the MO current in the range from 520 to 542 mA as a function of the PS current, while the optical power is fixed at 29.6 mW. We observed that such a condition requires that the PS current is adjusted step-by-step by following a linear trend. Hence, we imposed a linear fit to the data and a slope of a = 0.68 was obtained [25]. For the latter condition, the amplitude of the MO current modulation (ΔI_{MO}) and the amplitude of the PS current modulation (ΔI_{PS}) must satisfy the solution of the following pair of simultaneous equations:

$$\begin{cases} \Delta I_{PS} = a \cdot \Delta I_{MO} \\ \Delta I_{PS}{}^2 + \Delta I_{MO}{}^2 = b^2 \end{cases} \quad (6)$$

The solution is ΔI_{MO} = 2.2 mA and ΔI_{PS} = 1.6 mA. Figure 5b shows a QEPAS spectral scan that is acquired when a sinusoidal dither is applied with a modulation depth of 2.2 mA and 1.6 mA to the MO and PS sections, respectively, with the same initial phase. The phase section DC current was adjusted point-by-point, while MO DC current level is scanned.

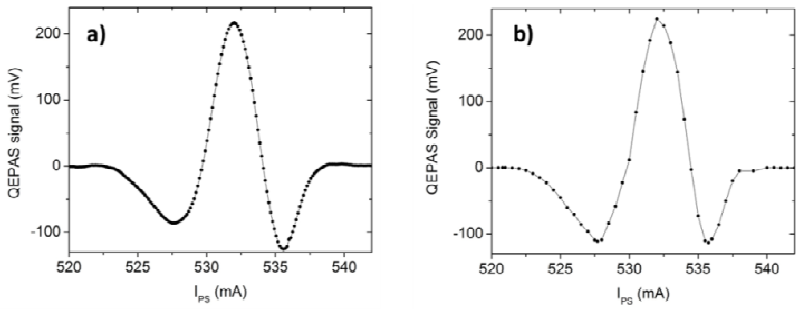

Figure 5. (a) QEPAS spectral scan of the selected N_2O absorption line with the QEPAS sensor operating in the WM mode and *2f*-detection. The current of the PS section was fixed at 120 mA while both a slow ramp at a frequency of 20 mHz and a sine frequency of 1435.88 Hz and amplitude of 2.7 mA were applied to the MO section. The integration time of the lock-in amplifier was set to 100 ms. (b) QEPAS spectral scan of the selected N_2O absorption line with the QEPAS sensor operating in a pure WM condition and *2f*-detection. The DC current of the PS section was adjusted point-by-point while the MO current varies from 520 mA to 542 mA in order to have a fixed optical power of 29.6 mW. A slow ramp at a frequency of 20 mHz was applied to applied to the MO section. A sine wave at a frequency of $f_o/2$=1435.88 Hz and amplitude of 2.2 mA and a sine wave at the same frequency and amplitude 1.6 mA were applied to the MO and PS section, respectively. The integration time of the lock-in amplifier was set to 100 ms.

As predicted, the *2f*-QEPAS signal shows a nearly pure second derivative of a Lorentzian line-shape, confirming that the RAM contribution was successfully suppressed.

5. PURE AMPLITUDE MODULATION

Pure AM spectroscopy occurs when the current modulation produces a modulation of the QCL intensity, but not a modulation of its wavelength as discussed in Section 2. In the three section QCL employed in this work, this approach can be accomplished by dithering the PS current with a sinusoidal waveform. In this case, the current modulation depth of the PS section allows both the switching between the QCL emission-on and -off during each oscillation as well as maximizing the QEPAS signal is 17.6 mA [23, 25]. A pure AM technique and *1f*-detection was implemented by applying a sinusoidal dither to the PS section at f_0 and demodulating the QEPAS signal at the same frequency. A ramp at a frequency of 20 mHz was applied to the MO section current in order to spectrally scan the selected absorption line. The spectral scans obtained at four different PS current values are shown in Figure 6.

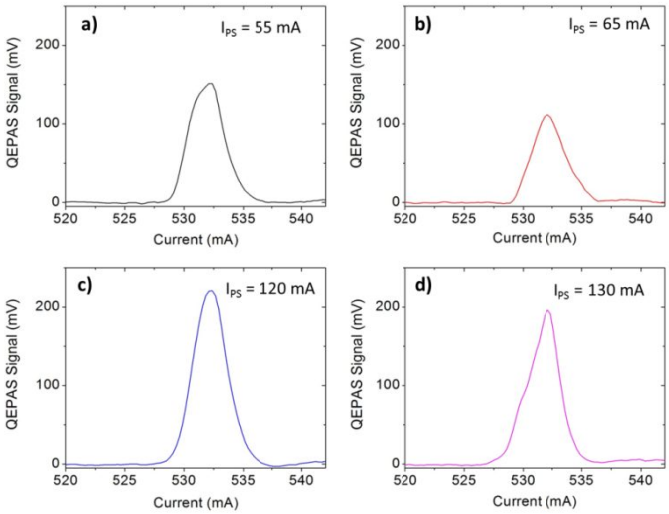

Figure 6. (a-d) QEPAS spectral scans of the selected N_2O absorption line with the QEPAS sensor operating in a pure AM condition with *1f*-detection. The DC PS current was set to 55 mA (a), 65 mA (b), 120 mA (c) and 130 mA (d). In all cases, the PS current was dithered with a sinusoidal waveform at f_0 and amplitude of 23.0 mA and a slow ramp at a frequency of 20 mHz was applied to theMO section in both cases. The integration time of the lock-in amplifier was set to 100 ms.

1f-QEPAS spectra show a background-free Voigt line-shape, demonstrating the achievement of a pure AM condition. The FWHM Lorentzian contribution to the Voigt fit for the spectrum at 120 mA is 0.0267 ± 0.0007 cm^{-1} [25], close to the pressure-broadening coefficient of 0.026 cm^{-1} in air for the operating pressure condition, as reported in the HITRAN database [24]. For these reasons, the pure AM technique can be used for gas sensing applications, especially for the detection of broadband absorbers, as well for investigations of absorption linewidth broadening phenomena in an unrelated gas matrix.

6. CONCLUSIONS

In this manuscript, we demonstrated the capability of a novel QCL structure composed by three different sections for pure amplitude and pure wavelength modulation spectroscopy targeting gas sensing applications. Both techniques have been investigated by using a QEPAS-based sensor. The structure of the QCL was designed in order to allow modulation of the laser wavelength while the optical power remains constant and, conversely, modulation of the optical power while the wavelength remains fixed. With pure amplitude modulation and *1f*-detection, we recovered the Voigt absorption line-shape of the selected N_2O absorption with a full-width-half-maximum value close to the pressure-broadening coefficient of 0.026 cm^{-1} reported in the HITRAN database. With pure wavelength modulation and *2f*-detection, a nearly pure second derivative line-shape of the absorption line was recorded without a RAM contribution.

ACKNOWLEDGEMENTS

Frank K. Tittel acknowledges support by the Welch Foundation (Grant R4925S). The authors from Dipartimento Interateneo di Fisica di Bari acknowledge financial support from two Italian research projects: PON02 00675 and PON02 00576.

REFERENCES

[1] Zhu, X., and Cassidy, D. T., "Modulation spectroscopy with a semiconductor diode laser by injection-current modulation," J. Opt. Soc. Am. B 14, 1945–1950 (1997).
[2] Kluczynski, P., and Axner, O., "Theoretical description based on Fourier analysis of wavelength-modulation spectrometry in terms of analytical and background signals," Appl. Opt. 38, 5803–5815 (1999).
[3] Schilt, S., Thévenaz, L., and Robert, P. , "Wavelength modulation spectroscopy: combined frequency and intensity laser modulation," Appl. Opt. 42, 6728–6738 (2003).
[4] Patimisco, P., Borri, S., Sampaolo, A., Beere, H. E., Ritchie, D. A., Vitiello, M. S., Scamarcio, G., and Spagnolo, V., "A quartz enhanced photo-acoustic gas sensor based on a custom tuning fork and a terahertz quantum cascade laser," Analyst, 139, 2079-2087 (2014).
[5] Schilt, S., Thévenaz, L., and Robert, P., "Wavelength modulation spectroscopy: combined frequency and intensity laser modulation," Appl. Opt. 42, 6728–6738 (2003).
[6] Duffin, K., McGettrick, A. J., Johnstone, W., Stewart, G., and Moodie, D. G., "Tunable diode laser spectroscopy with wavelength modulation: a calibration-free approach to the recovery of absolute gas absorption line shapes," J. Lightwave Technol. 25, 3114–3125 (2007).
[7] McGettrick, A. J., Duffin, K., Johnstone, W., Stewart, G., and Moodie, D. G., "Tunable diode laser spectroscopy with wavelength modulation: a phasor decomposition method for calibration-fee measurements of gas concentration and pressure," J. Lightwave Technol. 26, 432–440 (2008).
[8] Chakraborty, A. L., Ruxton, K., Johnstone, W., Lengden, M., and Duffin, K., "Elimination of residual amplitude modulation in tunable diode laser wavelength modulation spectroscopy using an optical fiber delay line," Opt. Express 17, 9602-9607 (2009).
[9] Li, L., Arsad, N., Stewart, G., Thursby, G., Culshaw, B., and Wang, Y., "Absorption line profile recovery based on residual amplitude modulation and first harmonic integration methods in photoacoustic gas sensing," Opt. Commun. 284, 312-316 (2011).
[10] Bain, J. R. P., Lengden, M., Stewart, G. and Johnstone, W., "Recovery of Absolute Absorption Line Shapes in Tunable Diode Laser Spectroscopy Using External Amplitude Modulation With Balanced Detection," IEEE Sens. J. 16, 675-680 (2016).

[11] Patimisco, P., Scamarcio, G., Tittel, F.K., Spagnolo, V., "Quartz-Enhanced Photoacoustic Spectroscopy: A Review," Sensors 14, 6165-6206 (2014).
[12] Kosterev, A.A., Tittel, F.K., Serebryakov, D., Malinovsky, A., and Morozov, A., "Applications of quartz tuning fork in spectroscopic gas sensing," Rev. Sci. Instrum. 76, 043105:1–043105:9 (2005).
[13] Wu, H., Sampaolo, A., Dong, L., Patimisco, P., Liu, X., Zheng, H., Yin, X., Ma, W., Zhang, L., Yin, W., Spagnolo, V., Jia, S., and Tittel, F. K., "Quartz enhanced photoacoustic H_2S gas sensor based on a fiber-amplifier source and a custom tuning fork with large prong spacing," Appl. Phys. Lett. 107, 111104 (2015).
[14] Sampaolo, A., Patimisco, P., Dong, L., Geras, A., Scamarcio, G., Starecki, T., Tittel, F. K., and Spagnolo, V., "Quartz-enhanced photoacoustic spectroscopy exploiting tuning fork overtone modes," Appl. Phys. Lett. 107, 231102 (2015).
[15] Zheng, H., Dong, L., Sampaolo, A., Wu, H., Patimisco, P., Yin, X., Ma, W., Zhang, L., Yin, W., Spagnolo, V., Jia, S., and Tittel, F. K., "Single-tube on-beam quartz-enhanced photoacoustic spectroscopy," Opt. Lett. 41, 978-981 (2016).
[16] Spagnolo, V., Patimisco, P., Pennetta, R., Sampaolo, A., Scamarcio, G., Vitiello, M. S., and Tittel, F. K., "THz Quartz-enhanced photoacoustic sensor for H_2S trace gas detection," Opt. Express 23, 7574-7582 (2015)
[17] Tittel, F.K., Sampaolo, A., Patimisco, P., Dong, L., Geras, A., Starecki, T., and Spagnolo, V., "Analysis of overtone flexural modes operation in quartz-enhanced photoacoustic spectroscopy," Opt. Express 24, A682-A692 (2016).
[18] Giglio, M., Patimisco, P., Sampaolo, A., Scamarcio, G., Tittel, F. K., and Spagnolo, V., "Allan Deviation Plot as a Tool for Quartz-Enhanced Photoacoustic Sensors Noise Analysis," IEEE Trans. Ultrason. Ferroelect. Freq. Control, 63, 555-560 (2016).
[19] Bidaux, Y., Terazzi, R., Bismuto, A., Gresch, T., Blaser, S., Muller, A., and Faist, J., "Measurements and simulations of the optical gain and anti-reflection coating modal reflectivity in quantum cascade lasers with multiple active region stacks," J. Appl. Phys. 118, 093101 (2015).
[20] Bismuto, A., Blaser, S., Terazzi, R., Gresch, T., and Muller, A., "High performance, low dissipation quantum cascade lasers across the mid-IR range," Opt. Express 23, 5477-5484 (2015).
[21] Bidaux, Y., Bismuto, A., Patimisco, P., Sampaolo, A., Gresch, T., Strubi, G., Blaser, S., Tittel, F. K., Spagnolo, V., Muller A., and Faist, J., "Mid infrared quantum cascade laser operating in pure amplitude modulation for background-free trace gas spectroscopy," Opt. Express 24, 26464- 26471 (2016).
[22] Patimisco, P., Sampaolo, A., Dong, L., Giglio, M., Scamarcio, G., Tittel, F.K., and Spagnolo, V., "Analysis of the electro-elastic properties of custom quartz tuning forks for optoacoustic gas sensing," Sensor Actuat. B-Chem. 227, 539-546 (2016).
[23] Zheng, H., Dong, L., Sampaolo, A., Wu, H., Patimisco, P., Ma, W., Zhang, L., Yin, W., Xiao, L., Spagnolo, V., Jia, S., and Tittel, F. K., "Overtone resonance enhanced single-tube on-beam quartz enhanced photoacoustic spectrophone," Appl. Phys. Lett. 109, 111103 (2016).
[24] Sampaolo, A., Patimisco, P., Giglio, M., Vitiello, M. S., Beere, H. E., Ritchie, D. A., Scamarcio, G., Tittel, F. K. and Spagnolo, V., "Improved Tuning Fork for Terahertz Quartz-Enhanced Photoacoustic Spectroscopy," Sensors, 16, 439 (2016).
[25] http://www.hitran.org/
[26] Patimisco, P., Sampaolo, A., Bidaux, Y., Bismuto, A., Scott, M., Jiang, J., Muller A., Faist, J., Tittel, F. K., and Spagnolo, V., "Purely wavelength- and amplitude-modulated quartz-enhanced photoacoustic spectroscopy," Opt. Express 24, 25943-25954 (2016).